Biochem. J. (2015) **466**, 163–176 (Printed in Great Britain) doi:10.1042/BJ20140428

Decreased adipogenesis and adipose tissue in mice with inactivated protein phosphatase 5

Wright Jacob*, Doron Rosenzweig*, Cristina Vázquez-Martin*, Suzanne L. Duce† and Patricia T. W. Cohen*[1]

*Medical Research Council Protein Phosphorylation and Ubiquitylation Unit, College of Life Sciences, University of Dundee, Dundee DD1 5EH, Scotland, U.K.
†Division of Biological Chemistry and Drug Discovery, College of Life Sciences, University of Dundee, Dundee DD1 5EH, Scotland, U.K.

Glucocorticoids play an important role in the treatment of inflammation and immune disorders, despite side effects, which include metabolic derangements such as central adiposity. These studies examine the role of protein phosphatase 5 (Ppp5) in glucocorticoid receptor (GR) complexes which mediate response to glucocorticoids. Mice homozygous for inactivated Ppp5 ($Ppp5^{D274A/D274A}$) exhibit decreased adipose tissue surrounding the gonads and kidneys compared with wild-type mice. Adipocyte size is smaller, more preadipocytes/stromal cell are present in their gonadal fat tissue and differentiation of preadipocytes to adipocytes is retarded. Glucocorticoid levels are raised and the GR is hyperphosphorylated in adipose tissue of $Ppp5^{D274A/D274A}$ mice at Ser212 and Ser220 (orthologous to human Ser203 and Ser211) in the absence of glucocorticoids. Preadipocyte cultures from $Ppp5^{D274A/D274A}$ mice show decreased down regulation of Delta-like protein-1/preadipocyte factor-1, hyperphosphorylation of extra-cellular signal regulated kinase 2 (ERK2) and increased concentration of (sex determining region Y)-box 9 (SOX9), changes in a pathway essential for preadipocyte differentiation, which leads to decreased concentrations of the transcription factors CEBPβ and CEBPα necessary for the later stages of adipogenesis. The data indicate that Ppp5 plays a crucial role in modifying GR-mediated initiation of adipose tissue differentiation, suggesting that inhibition of Ppp5 may potentially be beneficial to prevent obesity during glucocorticoid treatment.

Key words: glucocorticoid receptor, Hsp90, PP5, preadipocyte differentiation, preadipocyte factor-1, PPARγ.

INTRODUCTION

Glucocorticoids are widely used as drugs to control both acute and chronic inflammation and, at supraphysiological concentrations, they display strong immunosuppressive actions. Their use, however, is limited by side effects, which include metabolic derangements such as central obesity, glucose intolerance and insulin resistance, which are major risk factors for Type 2 diabetes and cardiovascular disease. Glucocorticoids exert their effect by binding to the glucocorticoid receptor (GR), a transcription factor which, on ligand binding, translocates from the cytoplasm to the nucleus, where it binds to specific sites in DNA and modulates the expression of many genes. The GR interacts with the chaperone heat shock protein (Hsp)90, which is involved in assembly and maturation of the GR and other steroid receptors [1]. Protein phosphatase 5 (Ppp5/PP5), which dephosphorylates serine and threonine residues in proteins [2,3], was identified as a component of GR-Hsp90 complexes [4,5] and shown to interact with Hsp90 and Hsp70 via its tetratricopeptide repeat (TPR) domain [6,7]. Three TPR-containing proteins, FK506 binding protein 51 (FKBP51), FKBP52 and Ppp5/PP5 are now known to separately associate with the mature GR through Hsp90, to form different GR complexes [8,9]. A further small protein termed p23 is an essential component of GR complexes [10]. Ppp5 is the only TPR protein that exhibits phosphatase activity in the GR complexes, and interaction of Ppp5 TPR domain with Hsp90 stimulates its protein phosphatase activity *in vitro* [11]. Ppp5 can also be activated *in vitro* by unsaturated and saturated fatty acids [12–14]. Studies in cell cultures have suggested that Ppp5 is a negative regulator of GR-mediated growth arrest [15] and that Ppp5 may modify the transcriptional profile of the cell [16]. However, analyses of two mouse models [17,18] where the expression of Ppp5/PP5 protein was below detection, termed PP5 'knockout' (KO) (PP5KO), did not report any overt *in vivo* physiological abnormalities attributed to alteration of GR function. In the present study, we analyse a murine model, in which an inactive Ppp5 replaces the wild-type Ppp5 and leads to changes in GR-mediated fat deposition. The studies demonstrate a major role of Ppp5 in preadipocyte differentiation.

MATERIALS AND METHODS

Generation and maintenance of $Ppp5^{D274\,A/+}$ and $Ppp5^{D274A/D274A}$ mice

All animal procedures were approved by the University of Dundee Ethical Committee and were performed under a UK Home Office Project Licence. Mice expressing the required Asp274Ala mutant Ppp5 were generated by ARTEMIS Pharmaceuticals. The targeting vector employed, encompassed exons 4–12 of the Ppp5 gene with a GAC→GCT codon change in exon 7 specifying the Asp274Ala substitution (Figure 1A). Neomycin (Neo) was used

Abbreviations: 11-β-HSD, 11-β-hydroxysteroid dehydrogenase; BAT, brown adipose tissue; CEB/P, CCAAT enhancer binding protein; CDC37, Hsp90 co-chaperone; DLK1, Delta-like protein-1; DMEM, Dulbecco's modified Eagle's medium; ERK/MAPK, extra-cellular signal regulated kinase/mitogen-activated protein kinases; ES, embryonic stem (cells); FA1, foetal antigen-1; FABP4, fatty acid binding protein 4; FAS, fatty acid synthase; FKBP, FK506 binding protein; Flpe, flippase; GAPDH, glyceraldehyde-3-phosphate dehydrogenase; GLUT4, glucose transporter; GR, glucocorticoid receptor; GTT, glucose tolerance test; HFD; high-fat diet; Hsp, heat shock protein; KI, knockin; KO, knockout; MEFs, mouse embryonic fibroblasts; PEPCK/PCK phosphoenolpyruvate carboxykinase; PPAR-γ, peroxisome proliferator-activated receptor-γ; Ppp5/PP5, protein phosphatase 5; Pref-1,Preadipocyte factor-1; SMAD3, mothers against decapentaplegic homologue 3; SOX9, (sex determining region Y)-box 9; TGF, transforming growth factor; TPR, tetratricopeptide repeat; UCP1, uncoupling protein-1; WAT, white adipose tissue.

[1] To whom correspondence should be addressed (email p.t.w.cohen@dundee.ac.uk).

for positive selection and thymidine kinase (TK) for negative selection. Upon homologous recombination, exons 4–12 of the endogenous Ppp5 gene (*PPP5 C*) were replaced with DNA encoding exons 4–6, exon 7 (with the GCT codon) and exons 8–12. C57BL/6 J genomic DNA was used for construction of the targeting vector, which was introduced into C57BL/6 N embryonic stem (ES) cells by electroporation. After selection in G418-containing medium, resistant clones were screened by PCR and Southern blotting, and cells from validated clones were injected into blastocytes, which were then transferred to the uteri of pseudopregnant foster mothers. Chimaeric male offspring were mated with female Flpe mice (animals coisogenic with C57BL/6 and containing a random integration of a CAGGS promoter-Flpe transgene, encoding a ubiquitous Flpe recombinase activity), allowing parallel *in vivo* Neo selection marker deletion and germ line transmission of the mutant GAC codon to the F1 offspring. Two mouse lines originating from different ES cell clones carrying the $Ppp5^{D274\,A}$ allele were maintained by backcrossing.

Preparation and culture of preadipocytes

Primary preadipocyte isolation and culture was modified from the method of [19]. Briefly, male or female mouse gonadal fat pads were excised in sterile conditions and approximately 0.5 mg placed in a 5 ml vial containing 1 ml of buffer comprising Krebs-Ringer buffer and HEPES [140 mM NaCl, 4.7 mM KCl, 2.5 mM $CaCl_2$, 1.25 mM $MgCl_2$, 2.5 mM NaH_2PO_4, 25 mM HEPES] with the addition of 3.5 % BSA (w/v), 2 mM glucose, 200 mM adenosine riboside (Fluka, Sigma–Aldrich) and 1 mg/ml collagenase type II (Worthington Biochemical Corp.) at room temperature. The adipose tissue was finely minced using scissors and incubated with the collagenase for 60 min at 37°C in a shaking water bath until fragments were no longer visible and the digest had a milky white appearance. Digests were filtered (BD Falcon cell strainer 70 μm) and centrifuged at 800 ***g*** for 10 min. The upper phase (floating adipocytes) was separated from lower phase. The lower phase was treated with red blood cell lysis buffer (Miltenyi Biotec) and centrifuged at 1000 ***g*** for 5 min. The upper phase was removed and the pellet containing stromal cells and preadipocytes was resuspended in RPMI-1640 medium (Life Technologies, Inc.) supplemented with 10 % FBS or 10 % dialysed FBS with molecules below 10 kDa removed (Biosera), 100 U/ml penicillin, 100 μg/ml streptomycin, 2 mM L-glutamine, 1 % non-essential amino acids (Life Technologies, Inc.), 1 % sodium pyruvate and 10 ng/ml mouse granulocyte-macrophage colony-stimulating factor (R&D Systems). The cells were plated at a density 1×10^6 in a 10 cm diameter dish, cultured until confluence was reached (2–4 days), then the medium was changed, with FBS being lowered to 5%, and the cells were cultured for a further 8–10 days in a humidified atmosphere with 5 % CO_2, 95 % air at 37°C. Preadipocytes were lysed as described for mouse embryonic fibroblasts (MEFs).

Statistical analysis

Where appropriate, data are presented $\pm$ the S.E.M. Statistical significance of the difference between the means of two data sets was assessed using Student's two tailed *t*-test unless otherwise stated.

RESULTS

Genetic and phenotypic analysis of $Ppp5^{+/+}$, $Ppp5^{D274\,A/+}$ and $Ppp5^{D274A/D274A}$ mice

Mutation of Asp274 to Ala in Ppp5 would be predicted to lead to inactivation because this amino acid is invariant throughout the PPP family phosphatases and forms a salt bridge with His304, which is required for donation of a hydrogen ion during cleavage of phosphate from the substrate [20]. GST-Ppp5 and GST-Ppp5(D274 A) generated in *Escherichia coli* showed similar expression levels and migration on SDS/PAGE (Figure S1C). Assay, after affinity purification on glutathione-Sepharose, indicated that the mutant Ppp5 was virtually inactive, expressing <0.27 % (± 0.12 % S.D.) of the wild-type Ppp5 activity. $Ppp5^{+/+}$, $Ppp5^{D274\,A/+}$ and $Ppp5^{D274A/D274A}$ mice, generated as described (Figure 1A, S1A and S1B), were viable, with no obvious phenotypic abnormalities at birth. Immunoblots of Ppp5 showed a band of the predicted size at 58 kDa in liver lysates of $Ppp5^{+/+}$ and $Ppp5^{D274A/D274A}$ mice. A cleaved Ppp5 band migrating at 50 kDa, believed to be a form involved in the activity and turnover of Ppp5 [7], was noted in $Ppp5^{+/+}$ mice but was absent from the $Ppp5^{D274A/D274A}$ liver lysates (Figure S1D).

Genetic analyses of the offspring of heterozygous ($Ppp5^{D274\,A/+}$) matings revealed a statistically significant decrease in the number of male $Ppp5^{D274A/D274A}$ mice born compared with the number expected (Figure 1B). The distribution of Ppp5 genotypes for the combined male and female offspring is significantly different from the expected distribution and there is a trend towards a decrease in the numbers of female $Ppp5^{D274A/D274A}$ mice (Figures S1E and S1F). There was also a trend towards significance for a decrease in the number of male and female $Ppp5^{D274A/D274A}$ embryos compared with the expected number (Figure 1C). Overall, these data suggest that $Ppp5^{D274A/D274A}$ mice expressing an inactive Ppp5 are selected against during prenatal development.

The weight of $Ppp5^{D274A/D274A}$ male mice increased more slowly than the weights of $Ppp5^{+/+}$ and $Ppp5^{D274\,A/+}$ male mice after 11 weeks of age (Figure 1D). An initial analysis of the internal organs of mice greater than 6 months old suggested that the gonadal and omental adipose tissue mass of $Ppp5^{D274A/D274A}$ mice was less than that of age- and gender-matched control animals. Dissection and weighing confirmed these observations in both male and female $Ppp5^{D274A/D274A}$ and $Ppp5^{D274\,A/+}$ mice (Figures 1E and S1G) and raised the question of whether slower expansion of adipose tissue may underlie or contribute to the differences in growth curves.

Fat depots of adult $Ppp5^{D274A/D274A}$ mice are decreased compared with those in wild-type mice

Central obesity is caused by an excess of abdominal (also termed visceral) adipose tissue, which comprises several fat depots including fat surrounding the kidneys, fat surrounding the gonads and fat at the front of the abdomen (omental fat) as well as between the organs in the abdomen (mesenteric fat). The kidneys and the adipose tissue surrounding the kidneys and gonads were examined by MRI. The volumes derived from the 3D MRI images for these tissues were then converted into weight as described in the Materials and methods section. Imaging of kidney and its associated adipose tissue demonstrated that these fat depots were significantly decreased in $Ppp5^{D274A/D274A}$ compared with $Ppp5^{D274\,A/+}$ and $Ppp5^{+/+}$ mice (Figures 2A–2C). The kidney fat and the kidney fat/kidney weight ratios showed a trend towards lower values in heterozygous $Ppp5^{D274\,A/+}$ mice compared with $Ppp5^{+/+}$ controls. Quantification of the kidney adipose depots by MRI directly correlated with data from manual weighing of the kidney fat pads (Figure 2D).

The images of the adipose tissue surrounding the gonads quantified by MRI show that the fat mass was decreased in $Ppp5^{D274\,A/+}$ mice compared with $Ppp5^{+/+}$ controls and markedly decreased in $Ppp5^{D274A/D274A}$ mice (Figure S2A). Although some

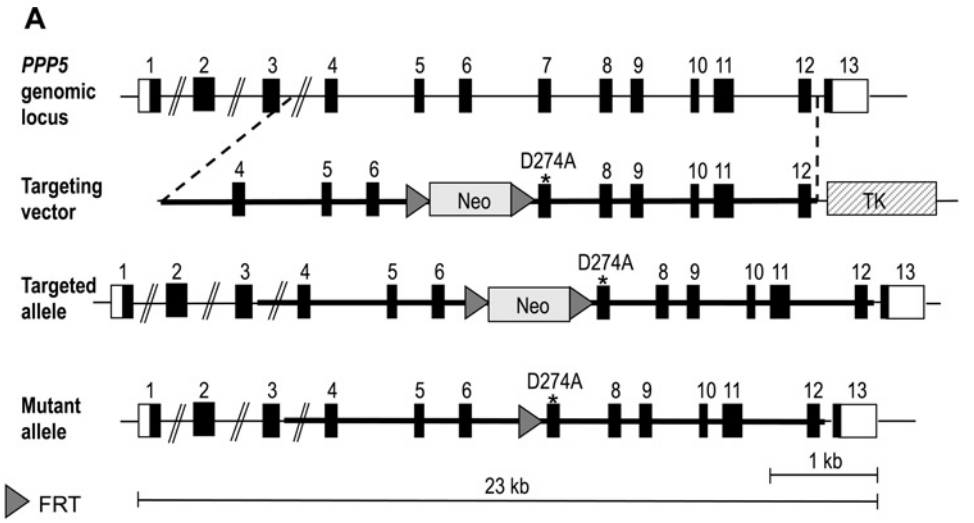

B

Genotype Male mice	Ppp5$^{+/+}$ Number (%)	Ppp5$^{D274A/+}$ Number (%)	Ppp5$^{D274A/D274A}$ Number (%)
Observed	66 (27.8)	134 (56.5)	37 (15.6)†
Expected	59 (25)	119 (50)	59 (25)

C

Genotype Embryos M + F	Ppp5$^{+/+}$ Number (%)	Ppp5$^{D274A/+}$ Number (%)	Ppp5$^{D274A/D274A}$ Number (%)
Observed	83 (32)	125 (48)	53 (20)
Expected	65 (25)	131 (50)	65 (25)

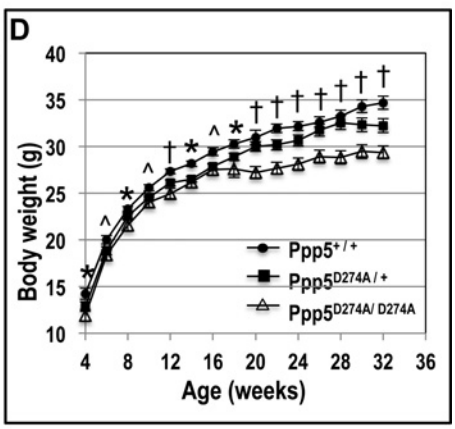

E

Male Genotype	Mice number	Age (weeks)	Body weight (g)	Liver weight (g)	Gonadal & omental fat (g)	Gonadal & omental fat/liver weight ratio
Ppp5$^{+/+}$	12	34.7±0.5	32.0±1.1	1.16±0.04	1.03±0.11	0.88±0.10
Ppp5$^{D274A/+}$	3	33.9±0.7	29.2±0.3	1.13±0.03	0.63±0.07 *	0.56±0.05
Ppp5$^{D274A/D274A}$	8	37.2±1.3	26.9±0.7 ***	1.04±0.05	0.44±0.05 ***	0.42±0.04 ***

Figure 1 Generation and genetically determined features of mice expressing an inactivated Ppp5

(**A**) Schematic representation of the generation of Ppp5$^{D274\,A}$ mutant allele in C57 BL/6 J mice as described in the Materials and methods section. (**B**) Genotype distribution of male offspring of Ppp5$^{D274\,A/+}$ heterozygous crosses. † The difference from the expected distribution is significant $P < 0.01$. (**C**) Genotype distribution of 13.5-day embryos of heterozygous crosses. (**D**) Growth curve for male mice of heterozygous crosses on a control diet. Increase in weight gain is significantly lower for Ppp5$^{D274A/D274A}$ mice than Ppp5$^{+/+}$ mice at all ages ($\wedge P < 0.05$, $^{*}P < 0.01$,†$P < 0.001$) and for Ppp5$^{D274\,A/+}$ mice compared with Ppp5$^{+/+}$ mice at weeks 12–16 ($P < 0.01$), weeks 18, 22 and 32 ($P < 0.05$). Numbers of mice weighed in different weeks Ppp5$^{+/+}$ (12–25), Ppp5$^{D274\,A/+}$ (16–35), Ppp5$^{D274A/D274A}$ (12–27). (**E**) Weight of adipose tissue (fat) dissected from the gonadal and omental fat depots of 7–9-month-old male Ppp5$^{+/+}$, Ppp5$^{D274\,A/+}$ and Ppp5$^{D274A/D274A}$ mice fed on a standard chow diet and compared with the liver weight. Statistically significant data: *** Ppp5$^{D274A/D274A}$ compared with Ppp5$^{+/+}$ $P < 0.002$, * Ppp5$^{D274A/D274A}$ compared with Ppp5$^{D274\,A/+}$ $P < 0.05$.

variation was observed, mostly in heterozygous mice, the data from weighing the gonadal fat directly correlated with the measurements generated by MRI, except in the case of a very large mouse (Figure S2B). This was probably due to the fat depots being partially squashed in the cradle holding the mouse in the MRI apparatus. Quantification of the liver volumes by MRI could not be achieved accurately, so the gonadal fat mass determined by MRI was therefore calculated as a ratio to the total body weight. The differences between the gonadal fat mass compared with the body weight in Ppp5$^{D274A/D274A}$ mice and Ppp5$^{D274\,A/+}$ compared with Ppp5$^{+/+}$ controls were statistically significant (Figure 2E). The age range of the mice over which this difference was examined and observed was 31.5–81 weeks, and it was present in two mouse lines originating from different ES cell clones carrying the Ppp5$^{D274\,A}$ allele.

Transverse sections of the abdomen showed that other white fat depots (subcutaneous fat and omental fat) were smaller in Ppp5$^{D274A/D274A}$ compared with Ppp5$^{+/+}$ mice (Figure S2A, bottom panel). However, our high-resolution MRI scanner produced images with a field of view of approximately 4 cm, and thus

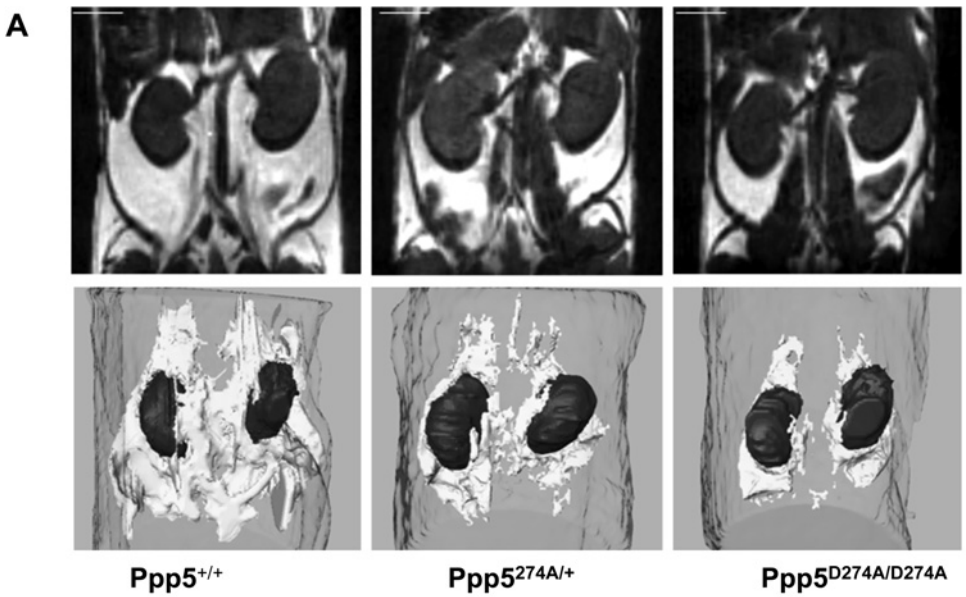

B

Genotype	Number of male mice	Age (weeks)	Body weight	Kidney weight MRI (g)	Kidney fat weight MRI (g)	Gonadal fat weight MRI (g)	Gonadal fat/body wt ratio	Kidney fat/kidney ratio
$Ppp5^{+/+}$	10	43.5±5.45	31.21±0.91	0.38±0.009	0.37±0.05	0.78±0.13	0.02±0.003	0.95±0.14
$Ppp5^{D274A/+}$	11	49.55±6.26	31.53±1.21	0.39±0.02	0.35±0.05	0.81±0.09	0.02±.002	0.8±0.14†
$Ppp5^{D274A/D274A}$	8	45.6±6.67	31.23±2.13	0.40±0.01	0.21±0.07	0.62±0.15	0.01±.003	0.46±0.1*

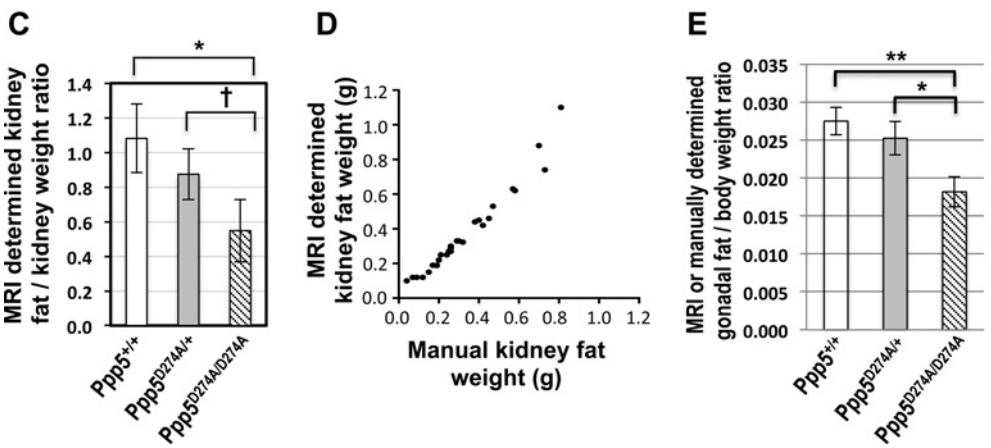

Figure 2 ***In vivo*** **quantification of the kidney fat pads in $Ppp5^{D274A/D274A}$, $Ppp5^{D274\,A/+}$ and $Ppp5^{+/+}$ mice by MRI**

(**A**) 2D frontal MR images (ventral view) of kidneys with 5 mm rulers (top row), and surface reconstructions of kidneys (black) and kidney fat pads (adipose tissue surrounding the kidney, white) (lower row) from 3D rapid acquisition relaxation enhanced (RARE)-4 MRI datasets of 81-week-old male mice. (**B**) Kidney, kidney and gonadal fat pads weights; volumes were determined by MRI and converted into grams. (**C**) Comparison of the kidney fat pad/kidney weight ratios in $Ppp5^{+/+}$, $Ppp5^{D274\,A/+}$ and $Ppp5^{D274A/D274A}$ mice. Statistically significant data using a one tailed *t*-test: *$Ppp5^{D274\,A/D274}$ compared with $Ppp5^{+/+}$ $P < 0.05$, †$Ppp5^{D274\,A/D274}$ compared with $Ppp5^{D274\,A/+}$ $P < 0.05$. (**D**) Correlation between the kidney fat weights determined *in vivo* by MRI and *ex vivo* by manual weighing in 29 male mice; $R^2 = 0.96$. (**E**) Comparison of the gonadal fat/body weight ratios determined by MRI or manual weighing in 22 $Ppp5^{+/+}$, 14 $Ppp5^{D274\,A/+}$ and 16 $Ppp5^{D274A/D274A}$ male mice. Ages were matched for the different genotypes and ranged from 31.5 to 81 weeks. Statistically significant data: **$Ppp5^{D274\,A/D274}$ compared with $Ppp5^{+/+}$ $P < 0.002$, *$Ppp5^{D274\,A/D274}$ compared with $Ppp5^{D274\,A/+}$ $P < 0.05$.

it was not possible to quantify the subcutaneous fat across the whole of the mouse. Nevertheless, inspection of the 3D MRI image data sets qualitatively suggests that the small size of fat depots in $Ppp5^{D274A/D274A}$ was not restricted to the gonadal or peri-renal fat.

Analysis of gonadal adipose tissue and preadipocyte differentiation in cultures from the adipose tissue

Haematoxylin–eosin staining of sections of the gonadal adipose tissue showed that in a small field of view of constant area

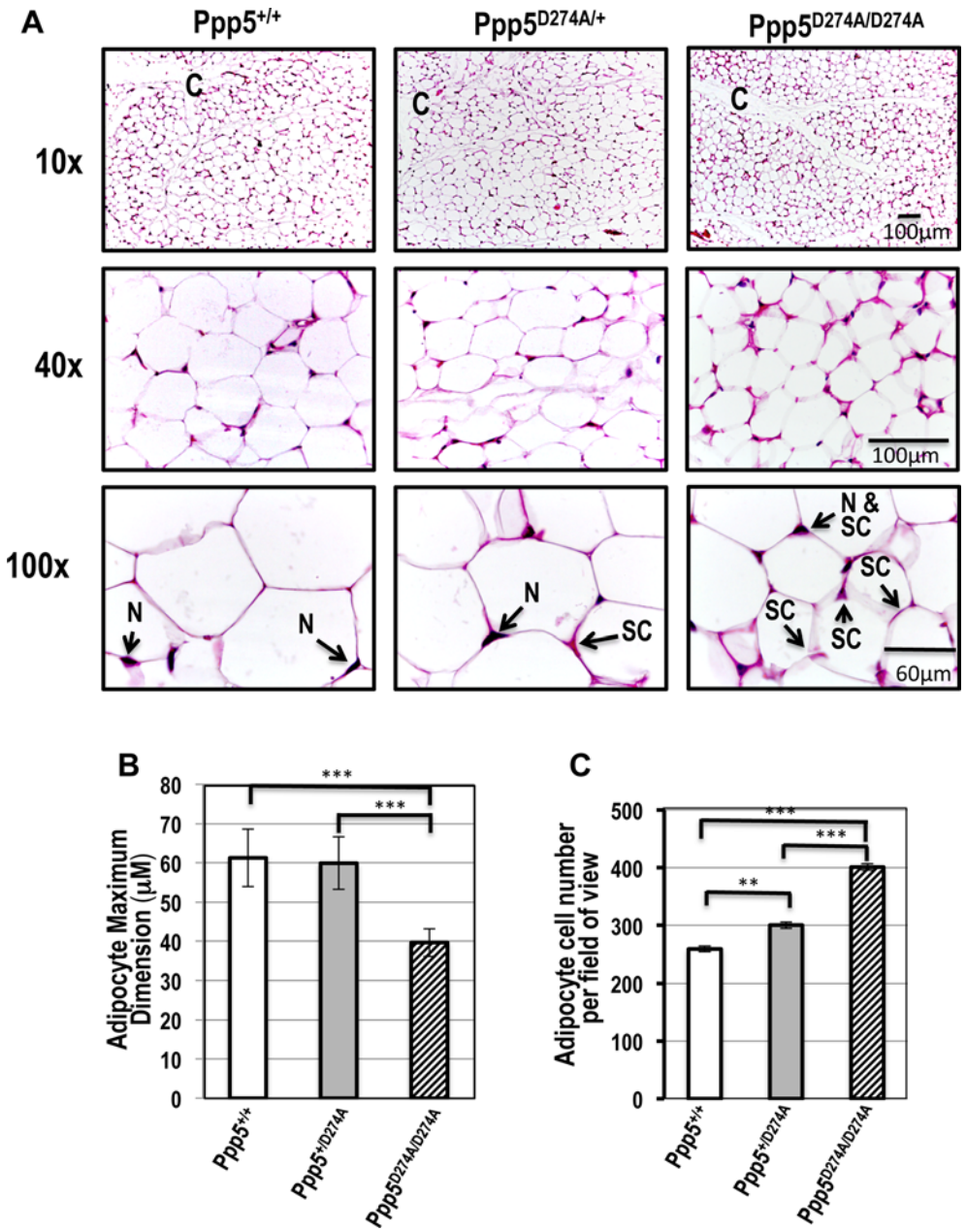

Figure 3 Comparison of gonadal adipose tissue sections from Ppp5$^{+/+}$, Ppp5$^{D274A/+}$ and Ppp5$^{D274A/D274A}$ mice

(**A**) Sections of gonadal adipose tissue fixed and stained with haematoxylin-eosin to visualize the adipocyte nuclei (dark blue, labelled N) and preadipocyte/stromal cell cytoplasm (labelled SC and visualized as pink on the original images). The stain is excluded from the lipid droplets. Blood capillaries (C) are indicated. The sections were imaged at magnifications of 10×, 40× and 100×. (**B**) Mean dimension of >70 adipocytes for each mouse genotype, determined by measuring the maximum dimension of adipocytes visible in a field of view. Error bars indicate the SEM and statistical significance is $***P < 10^{-13}$. Tissue sections from three mice of each genotype showed similar results (**C**) Adipocytes were counted in three fields of view of the same area for each mouse genotype indicated. Error bars indicate the SEM and statistical significance is $**P < 0.0005$, $***P < 10^{-8}$.

and magnification, the sizes of the adipocytes are significantly smaller in Ppp5$^{D274A/D274A}$ than in Ppp5$^{D274A/+}$ mice and Ppp5$^{+/+}$ controls (Figures 3A and 3B). Therefore, the number of adipocytes is higher in the Ppp5$^{D274A/D274A}$ field of view (Figure 3C) but not in the entire gonadal fat pads because the weight of the gonadal fat pads is lower in Ppp5$^{D274A/D274A}$ than in heterozygous and control mice. Importantly, more stromal cells are visible at the junctions between adipocytes in Ppp5$^{D274A/D274A}$ mice than in heterozygous or control mice (Figure 3A, 100× magnification). The observations suggest there may be a partial defect in the generation of adipocytes and subsequent accumulation of lipids in Ppp5$^{D274A/D274A}$ mice.

To investigate the biochemical changes in adipose tissue of Ppp5 deficient mice, preadipocytes were prepared from the adipose tissue surrounding the gonads by digestion with collagenase. The fraction containing the stromal cells and preadipocytes was cultured in fresh RPMI medium containing 10% complete FBS until confluence (2 days) and then replated in fresh medium containing 5% complete FBS and cultured for a further 8 days. Ppp5$^{+/+}$ cultures contained significantly

more differentiated adipocytes compared with $Ppp5^{D274A/D274A}$ and $Ppp5^{D274\,A/+}$ cultures ($P < 0.01$) as judged by staining with Nile Red, which detects intracellular lipid droplets (Figures 4A and 4B). When the stromal cell/preadipocyte fraction was plated similarly but cultured in RPMI medium containing dialysed FBS (to remove glucocorticoids and other molecules below 10 kDa), the cells were slower to reach confluence (4 days) and the differences in differentiation between $Ppp5^{+/+}$ controls and $Ppp5^{D274\,A/+}$ and $Ppp5^{D274A/D274A}$ cells was more pronounced ($P < 0.005$) (Figure 4C). In RPMI medium/dialysed FBS, there was a 10-fold difference in the number of $Ppp5^{+/+}$ and $Ppp5^{D274A/D274A}$ differentiated adipocytes, whereas in RPMI/complete FBS the difference was only 2-fold (compare Figures 4B and 4C). Overall, the data show that $Ppp5^{D274A/D274A}$ and $Ppp5^{D274\,A/+}$ preadipocytes differentiate more slowly than preadipocytes from $Ppp5^{+/+}$ controls, particularly in media depleted of glucocorticoids.

Whole body biochemical analyses of $Ppp5^{D274A/D274A}$ and $Ppp5^{D274\,A/+}$ mice

There was no significant difference between the fasting blood glucose levels of $Ppp5^{D274A/D274A}$ and $Ppp5^{D274\,A/+}$ and $Ppp5^{+/+}$ mice, but following an intraperitoneal injection of a bolus of glucose, $Ppp5^{D274A/D274A}$ and $Ppp5^{D274\,A/+}$ mice exhibited a slightly but significantly more rapid clearance of glucose from the blood when compared with $Ppp5^{+/+}$ controls (Figure 4D). The clearance of glucose from the blood after an intraperitoneal injection of a bolus of insulin was also slightly more rapid in $Ppp5^{D274A/D274A}$ and $Ppp5^{D274\,A/+}$ mice than in $Ppp5^{+/+}$ controls (Figure S3A).

In order to examine whether inhibition of Ppp5 might be a useful pharmaceutical target for management of diet-induced obesity, mice were fed a high-fat diet (HFD), containing 45 kcal % fat (1 cal = 4.184 J). As observed with mice fed the control diet, $Ppp5^{D274A/D274A}$ gained weight more slowly than $Ppp5^{D274\,A/+}$ and $Ppp5^{+/+}$ mice on the HFD (Figure S3B). However, the ratio of the weight gain of $Ppp5^{D274A/D274A}$, $Ppp5^{D274\,A/+}$ and $Ppp5^{+/+}$ mice after the HFD for 20 weeks to the weight gain after the control diet for 20 weeks was 2.2, 2.2 and 1.9, respectively, indicating that $Ppp5^{D274\,A/D274A}$ and $Ppp5^{D274\,A/+}$ mice are susceptible to increased weight gain on a HFD. Indeed glucose tolerance tests (GTT) showed that after glucose administration, the blood glucose levels of $Ppp5^{D274A/D274A}$ and $Ppp5^{D274\,A/+}$ mice returned to their basal levels slightly but significantly more slowly than those in $Ppp5^{+/+}$ mice (Figure S3C). No significant differences were observed between the three Ppp5 mouse genotypes, which all showed resistance to insulin (data not shown). On termination of the HFD, the weight ratio of gonadal and omental fat to liver was higher in $Ppp5^{D274A/D274A}$ and $Ppp5^{D274\,A/+}$ mice than in control $Ppp5^{+/+}$ mice (Figure S3D). The studies demonstrate that inhibition of Ppp5 activity does not protect against HFD-diet-induced weight gain and fat deposition in mice.

Triacylglycerols (triglycerides) and glucocorticoids were measured in blood serum. In fasted male mice, triacylglycerols were significantly lower in $Ppp5^{D274A/D274A}$ compared with $Ppp5^{+/+}$ mice ($P < 0.001$) and $Ppp5^{D274\,A/+}$ mice compared with $Ppp5^{+/+}$ controls ($P < 0.01$), indicating improved lipid homoeostasis. This is likely to arise because the amounts of white adipose tissue (WAT) are too low to maintain normal fasted blood serum triacylglycerol levels. In fed mice, there were no statistically significant differences, although there was a trend towards higher levels in the $Ppp5^{D274A/D274A}$ mice compared with $Ppp5^{+/+}$ controls, suggesting dietary lipids were not being stored as rapidly in the Ppp5 mutant mice because of smaller white fat depots (Figure 4E). The levels of glucocorticoids were significantly higher in male fasted $Ppp5^{D274A/D274A}$ and $Ppp5^{D274\,A/+}$ mice than in $Ppp5^{+/+}$ controls ($P < 0.001$; $P < 0.04$), and in female fasted $Ppp5^{D274A/D274A}$ mice than in $Ppp5^{+/+}$ controls ($P < 0.03$) (Figure 4F), but there were no statistically significant differences in male or female fed mice (data not shown).

Examination of the phosphorylation state of GR–Hsp90 complexes in $Ppp5^{+/+}$, $Ppp5^{D274\,A/+}$ and $Ppp5^{D274A/D274A}$ mice

In mice, the major active glucocorticoid is corticosterone, which binds to and activates GR complexes to modulate the expression of many genes. If GR function is impaired in Ppp5 mutant mice, it is envisaged that this may enhance not only the conversion of the inactive 11-dehydrocorticosterone into corticosterone but also glucocorticoid release into the blood plasma from the adrenal. The elevated levels of serum glucorticoids in $Ppp5^{D274A/D274A}$ mice therefore suggested that GR function may be impaired in Ppp5 mutant mice and raised the possibility that GR phosphorylation state may be altered. The GR protein was difficult to detect in adipose tissue or MEF lysates and therefore the GR and its phosphorylation sites for which antibodies are available were examined after immunoadsorption of the GR in the absence and presence of the synthetic glucocorticoid, dexamethasone, a high-potency ligand for GR. Immunoblotting of anti-GR antibody pellets from MEF lysates shows increased levels of phosphorylation on GRSer212 and GRSer220 in the mutant mice (sites orthologous to human GRSer203 and GRSer211, respectively). GRpSer212 was increased in $Ppp5^{D274A/D274A}$ compared with $Ppp5^{+/+}$ MEFs in the absence of dexamethasone (Figure 5A). Three different animals of each genotype were examined and the difference was statistically significant ($P < 0.001$). GRpSer220 was also hyperphosphorylated in $Ppp5^{D274A/D274A}$ compared with $Ppp5^{+/+}$ cells in the absence of dexamethasone (Figure 5B). The similar levels of GRpSer220 in untreated and dexamethasone treated $Ppp5^{D274A/D274A}$ MEFs are consistent with GRpSer220 being hyperphosphorylated in the absence of dexamethasone. Quantification by the Li-Cor Odyssey detection system shows that in the absence of dexamethasone, the GRpSer220/GR phosphorylation ratio is increased approximately 10-fold in $Ppp5^{D274A/D274A}$ MEFs compared with the GRpSer220/GR ratio in $Ppp5^{+/+}$ MEFs (Figure 5C). Treatment with dexamethasone increases the GRpSer220/GR ratio 18-fold in $Ppp5^{+/+}$ MEFs, whereas there is a 5-fold increase in $Ppp5^{D274\,A/+}$ MEFs and only a marginal increase in $Ppp5^{D274A/D274A}$ MEFs compared with the levels in untreated MEFs (Figure 5C). The reason for lower GRp220/GR ratios in $Ppp5^{D274A/D274A}$ and $Ppp5^{D274\,A/+}$ compared with $Ppp5^{+/+}$ MEFs in the presence of dexamethasone is unclear, but could be due to the degradation of GRpSer220 when it cannot be dephosphorylated.

As expected Hsp90 and Ppp5 are present in GR immunopellets from preadipocyte lysates (Figure 5D) and MEF lysates. Following electrophoretic separation of the proteins in GR immunopellets from MEF lysates (data not shown), analysis by mass spectrometry identified Hsp90AB (orthologous to human Hsp90β) as the only Hsp90 isoform in the GR from both $Ppp5^{+/+}$ and $Ppp5^{D274A/D274A}$ MEFs. The Hsp90 co-chaperone Cdc37, phosphorylated *in vivo* on Ser13, is reported to be dephosphorylated by Ppp5 [21]. However, we did not observe a significant difference in the phosphorylation state of Cdc37 at Ser13 in $Ppp5^{D274A/D274A}$, $Ppp5^{D274\,A/+}$ and $Ppp5^{+/+}$ in MEF lysates (data not shown). PPARγ (peroxisome proliferator-activated

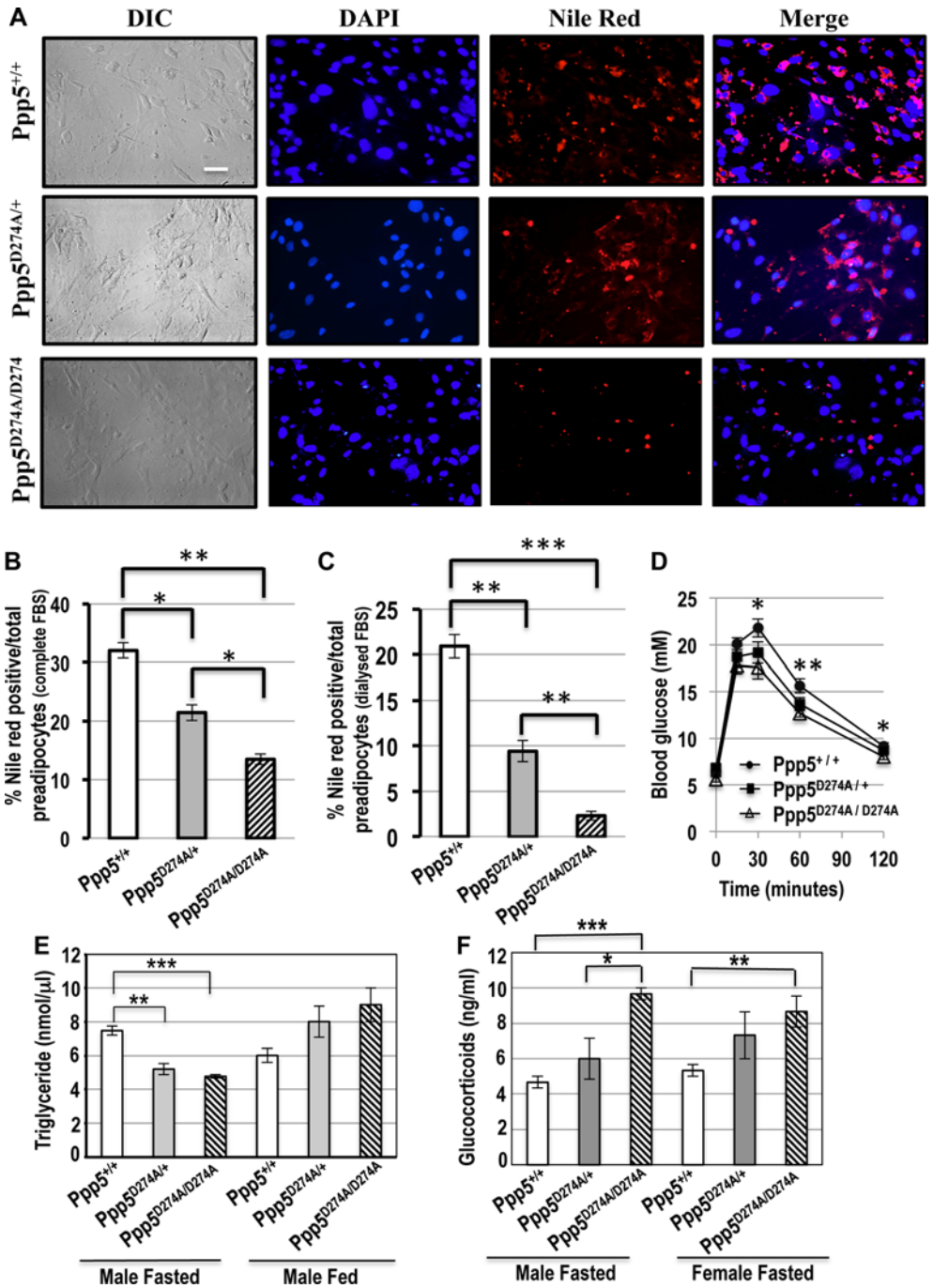

Figure 4 Differentiation of preadipocytes from Ppp5$^{+/+}$, Ppp5$^{D274A/+}$ and Ppp5$^{D274A/D274A}$ mice and blood serum glucose, triacylglycerol and glucocorticoid levels

(**A**) Preadipocytes isolated from gonadal fat were cultured for 10 days in RPMI medium containing complete FBS (with one passage), fixed in *p*-formaldehyde and initially viewed using differential interference contrast (DIC). DNA was stained with DAPI (blue), fat droplets with Nile Red and the merged images are shown on the right for all three genotypes as indicated. (**B, C**) Two hundred cells were scored for DAPI staining (preadipocyte total) and Nile Red (presence of fat droplets) in cultures grown in (**B**) RPMI medium (with complete FBS) (**C**) RPMI medium (with dialysed FBS, molecules <10 kDa removed). The presence of differentiated adipocytes indicated by fat droplets was significantly higher in Ppp5$^{+/+}$ cultures than in Ppp5$^{D274A/+}$ and Ppp5$^{D274A/D274A}$ cultures. Preadipocytes cultured from three mice of each genotype showed similar results. Error bars indicate the SEM and statistical significance by $^{*}P < 0.01$, $^{**}P < 0.005$, $^{***}P < 0.0005$. (**D**) Glucose tolerance test on 33–41-week-old male mice fed *ad libitum* on a standard chow diet and fasted (12 h) prior to the tests (8 Ppp5$^{D274A/D274A}$, 9 Ppp5$^{D274A/+}$, 12 Ppp5$^{+/+}$ mice). Ppp5$^{D274A/D274A}$ mice showed a small increase in glucose tolerance compared with Ppp5$^{+/+}$ mice, which was statistically significant at the 30 min, 120 min ($^{*}P < 0.05$) and 60 min ($^{**}P < 0.01$) time points post glucose injection. (**E**) Serum triacylglycerol (triglyceride) and (**F**) glucocorticoids were measured in blood serum from three male or three female, fed or fasted for 6 h Ppp5$^{D274A/D274A}$, Ppp5$^{D274A/+}$ and Ppp5$^{+/+}$ mice between 3.5 and 8 months old (but age-matched for genotypes). The blood serum triacylglycerol levels were decreased in fasted male Ppp5$^{D274A/D274A}$ compared with Ppp5$^{+/+}$ mice $^{***}P < 0.001$ and Ppp5$^{D274A/+}$ compared with Ppp5$^{+/+}$ mice $^{**}P < 0.01$. The glucocorticoid level was significantly higher in male fasted Ppp5$^{D274A/D274A}$ mice than in Ppp5$^{+/+}$ controls $^{***}P < 0.001$, female fasted Ppp5$^{D274A/D274A}$ mice than in Ppp5$^{+/+}$ controls $^{**}P < 0.03$ and in male fasted Ppp5$^{D274A/+}$ mice than in Ppp5$^{+/+}$ controls $^{*}P < 0.04$. Serum glucocorticoid levels in fed male and female mice was below 0.8 ng/ml.

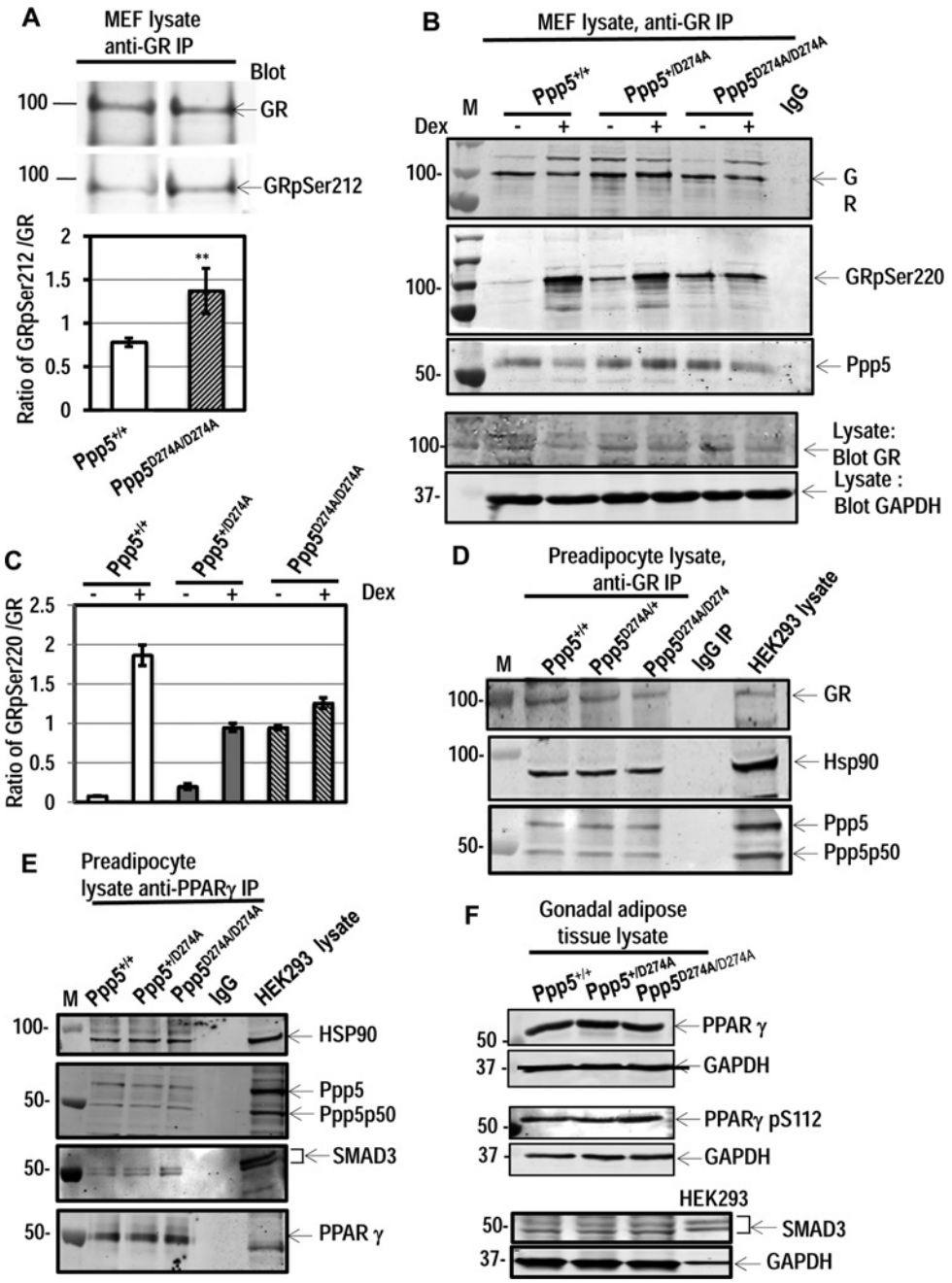

Figure 5 Analysis of GR complexes in MEFs and preadipocytes and PPARγ complexes in adipose tissue from Ppp5$^{+/+}$, Ppp5$^{D274\,A/+}$ and Ppp5$^{D274A/D274A}$ mice

(**A**) MEFs were cultured in DMEM and dialysed FBS. GR complexes were immunoadsorbed from Ppp5$^{+/+}$ and Ppp5$^{D274A/D274A}$ MEF lysates and immunoblotted for the GR and GRpSer212 (orthologous to human GRpSer203). Marker protein sizes on the left in kDa. A representative blot of three independent experiments is shown. Below, the data were averaged from the three blots. Error bars indicate the SEM and the difference is statistically significant ($P < 0.001$). (**B**) MEFs were cultured in DMEM and dialysed FBS with and without 500 nM dexamethasone (Dex) for 4 h. The GR was immunoadsorbed and blotted for the GR and GRpSer220 (orthologous to human GRpSer211). Ppp5 in the GR complexes is shown. IgG replacing the anti-GR employed for immunoadsorption served as a control for non-specific adsorption. GAPDH and the GR present in the lysate prior to immunoadsorption are controls. M, marker proteins in kDa. (**C**) Quantification of the data from (**B**) showing GR Ser220 is hyperphosphoryled in Ppp5$^{D274\,A/+}$ and Ppp5$^{D274A/D274A}$ MEFs compared with Ppp5$^{+/+}$ MEFs from the untreated cultures, but not in dexamethasone treated cells. Error bars relate to Li-Cor Odyssey quantifications. Similar hyperphosphorylation of GR Ser220 was noted in three independent experiments. (**D**) Preadipocytes were cultured in DMEM and dialysed FBS. The GR complexes were immunoadsorbed from the lysates and the proteins identified in the pellets by immunoblotting are indicated. The HEK293 lysate facilitates identification of the preadipocyte proteins. M, marker proteins in kDa. (**E**) PPARγ complexes were immunoadsorbed from the preadipocyte lysates and the proteins identified in the pellets by immunoblotting are indicated. IgG replacing the anti-PPARγ employed for immunoadsorption served as a control for non-specific adsorption. (**F**) Lysates from gonadal fat pads are examined by immunoblotting with antibodies to the indicated proteins.

receptor-γ) plays a key role in lipid accumulation [22] and binds to Hsp90 and Ppp5 in preadipocyte lysates (Figure 5E). PPARγ is reported to be regulated by dephosphorylation of phosphoSer112 by Ppp5 [23]. However, there was no significant difference in the phosphorylation of PPARγ Ser112 (orthologous to human Ser 114) in gonadal adipose tissue lysates from Ppp5$^{D274A/D274A}$, Ppp5$^{D274A/D274A}$ and Ppp5$^{+/+}$ mice (Figure 5F).

The GR has been shown to bind and inhibit mothers against decapentaplegic homologue 3 (SMAD3), which is an intracellular signal transducer relaying the transforming growth factor (TGF)-β signal to the nucleus from the TGF-β receptor kinase in the cell membrane [24]. The GR immunoadsorbed from preadipocyte lysates of gonadal fat pads of Ppp5$^{+/+}$ Ppp5$^{D274\,A/+}$ and Ppp5$^{D274A/D274A}$ mice interacted with the same amounts of SMAD3 and SMAD3 phosphorylated on Ser243 and Ser245 (data not shown). PPARγ immunoadsorbed from the preadipocyte lysates was also observed to bind SMAD3 (Figure 5E). However, the SMAD3 bound to PPARγ, and the levels present in gonadal adipose tissue lysates (Figure 5F) were the same in Ppp5$^{+/+}$ Ppp5$^{D274\,A/+}$ and Ppp5$^{D274A/D274A}$ mice.

Investigation of proteins regulating preadipocyte differentiation

Glucocorticoids have been shown to play a major role in differentiation of preadipocytes to adipocytes by decreasing transcription of the mRNA encoding Delta-like protein-1 (DLK1)/Preadipocyte factor-1 (Pref-1)/foetal antigen-1(FA1), in the early stages of preadipocyte differentiation [25,26]. In order to examine the effect of an inactive Ppp5 on this pathway, DLK1 and other proteins identified in the regulation of adipogenesis were investigated in predipocytes isolated from gonadal adipose tissue of mice expressing active and inactive Ppp5. Immunoblotting of lysates of preadipocytes, isolated from gonadal fat pads and cultured *in vitro* for 9 days showed that DLK1 was increased in level in Ppp5$^{D274\,A/+}$ and Ppp5$^{D274A/D274A}$ cells compared with Ppp5$^{+/+}$ cells, indicating that transcription of DLK1 mRNA was not being repressed by the GR when Ppp5 was inactivated (Figures 6A and 6B). From studies in Pref1/DLK1 null mice, DLK1 was shown to induce expression of the transcription factor (sex determining region Y)-box 9 (SOX9) through activation of the extra-cellular signal regulated kinase (ERK)/mitogen-activated protein kinases (MAPK) pathway, leading to inhibition of forced adipocyte differentiation in MEFs, by repression of CCAAT enhancer binding protein-β (C/EBPβ) and C/EBPδ [27,28]. In Ppp5$^{D274\,A/+}$ and Ppp5$^{D274A/D274A}$ preadipocyte cultures, the concentration of SOX9 was increased compared with that in Ppp5$^{+/+}$ preadipocyte cultures, whereas the glyceraldehyde-3-phosphate dehydrogenase (GAPDH) control did not vary (Figures 6A and 6B). Phosphorylated ERK2 was increased in Ppp5$^{D274A/D274A}$ compared with Ppp5$^{+/+}$ preadipocytes. The concentration of C/EBPβ, and that of C/EBPα which regulates terminal adipocyte differentiation [29,30], were decreased in Ppp5$^{D274\,A/+}$ and Ppp5$^{D274A/D274A}$ compared with Ppp5$^{+/+}$ preadipocyte lysates. C/EBPδ and PPARγ were below the level of detection in preadipocyte lysates.

The concentrations of fatty acid binding protein 4 (FABP4) involved in the uptake and transport of fatty acids, fatty acid synthase (FAS) and phosphoenolpyruvate carboxykinase (PEPCK/PCK), a regulator of gluconeogenesis, were similar in preadipocyte lysates from Ppp5$^{+/+}$ Ppp5$^{D274\,A/+}$ and Ppp5$^{D274A/D274A}$ mice (Figure 6C). The concentration of the glucose transporter (GLUT4) was sometimes slightly increased in Ppp5$^{D274\,A/+}$ and Ppp5$^{D274A/D274A}$ compared with Ppp5$^{+/+}$ preadipocytes (data not shown) but also observed at similar levels in other preadipocyte cultures of all three genotypes (Figure 6C). Other proteins relevant to lipid metabolism were examined in the adipose tissue surrounding the gonads. No changes in expression levels of 11-β-hydroxysteroid dehydrogenase (11-β-HSD1), adiponectin and perilipin were observed (Figure 6D). Visual examination of tissues did not suggest that lipid levels were increased in Ppp5$^{D274A/D274A}$ to compensate for the decreased lipid stored in white gonadal and peri-renal adipose tissue. In addition, measurement of lipids in the liver showed no significant difference between the livers of three paired Ppp5$^{D274A/D274A}$ and Ppp5$^{+/+}$ mice (Average 8.5 v 8.3% lipid/g respectively with $\leqslant$5 % difference between each pair of mice).

As the lower body mass of Ppp5$^{D274A/D274A}$ compared with Ppp5$^{+/+}$ cannot simply be explained by decreased adipogenesis but necessitates some change in energy intake or expenditure, tests were undertaken to address this point. However, no statistically significant difference in standard chow intake was observed between four Ppp5$^{D274A/D274A}$, three Ppp5$^{D274\,A/+}$ and three Ppp5$^{+/+}$ 12-week-old female mice when food was weighed every 2 days over 2 weeks [average (g) 50.5 ± 0.4, 52.2 ± 1.1, 54.0 ± 3.0, respectively]. The high level of glucocorticoids in the blood suggested the possibility that the expression of UCP1 (uncoupling protein-1) may be modified in Ppp5$^{D274A/D274A}$ mice resulting in loss of energy through heat generation [31], but analyses showed no increase of expression in UCP1 in brown adipose tissue (BAT) and no UCP1 expression in white gonadal tissue from three Ppp5$^{D274A/D274A}$ mice, which would suggest the presence brite/beige adipose tissue or adipocytes in this fat depot of Ppp5$^{D274A/D274A}$ mice (Figure 6E).

DISCUSSION

The mouse model we have engineered here, in which the wild-type Ppp5 gene is replaced by a gene expressing a Ppp5 protein with severely deficient activity, exhibits a major phenotype of decreased adipose tissue surrounding gonads and kidneys, and a reduction in size of the adipocytes present. The decrease in adipose tissue, evident by weighing, correlated well with data obtained by MRI. Our biochemical analyses, including elevated serum glucorticoids, suggest that the primary defect underlying this phenotype may be an alteration in GR function during the early stages of adipose tissue differentiation from preadipocytes. We demonstrate that preadipocytes expressing inactivated Ppp5 differentiate more slowly in culture than in wild-type preadipocytes and that more stromal cells, which include preadipocytes, are present in the gonadal fat pads of Ppp5$^{D274A/D274A}$ mice, data which support a block in an early step of preadipocyte differentiation. Two mouse PP5KO models were previously analysed without noting decreased amounts of adipose tissue or biochemical alterations in this tissue [17,18]. Our studies on the Ppp5$^{D274\,A}$ 'knockin' (KI) (Ppp5KI) mouse are the first to report the effects of inactivated Ppp5 on GR phosphorylation and differentiation in adipose tissue of an animal model. Homozygous Ppp5KI and PP5KO mice were viable and fertile, but selection against the homozygous male offspring of Ppp5KI heterozygous intercrosses was statistically significant and a similar prenatal effect was observed in one of the KO models [18]. Our genetic analyses further show that there is a trend towards significance for selection against homozygous Ppp5KI female offspring and 13.5-day male/female embryos of Ppp5$^{D274\,A/+}$ intercrosses. These analyses indicate a major role for Ppp5 before birth and are consistent with modulation of the GR, which is essential for early development [32].

Three conserved serine residues are known to be phosphorylated within the N-terminal region of the GR and

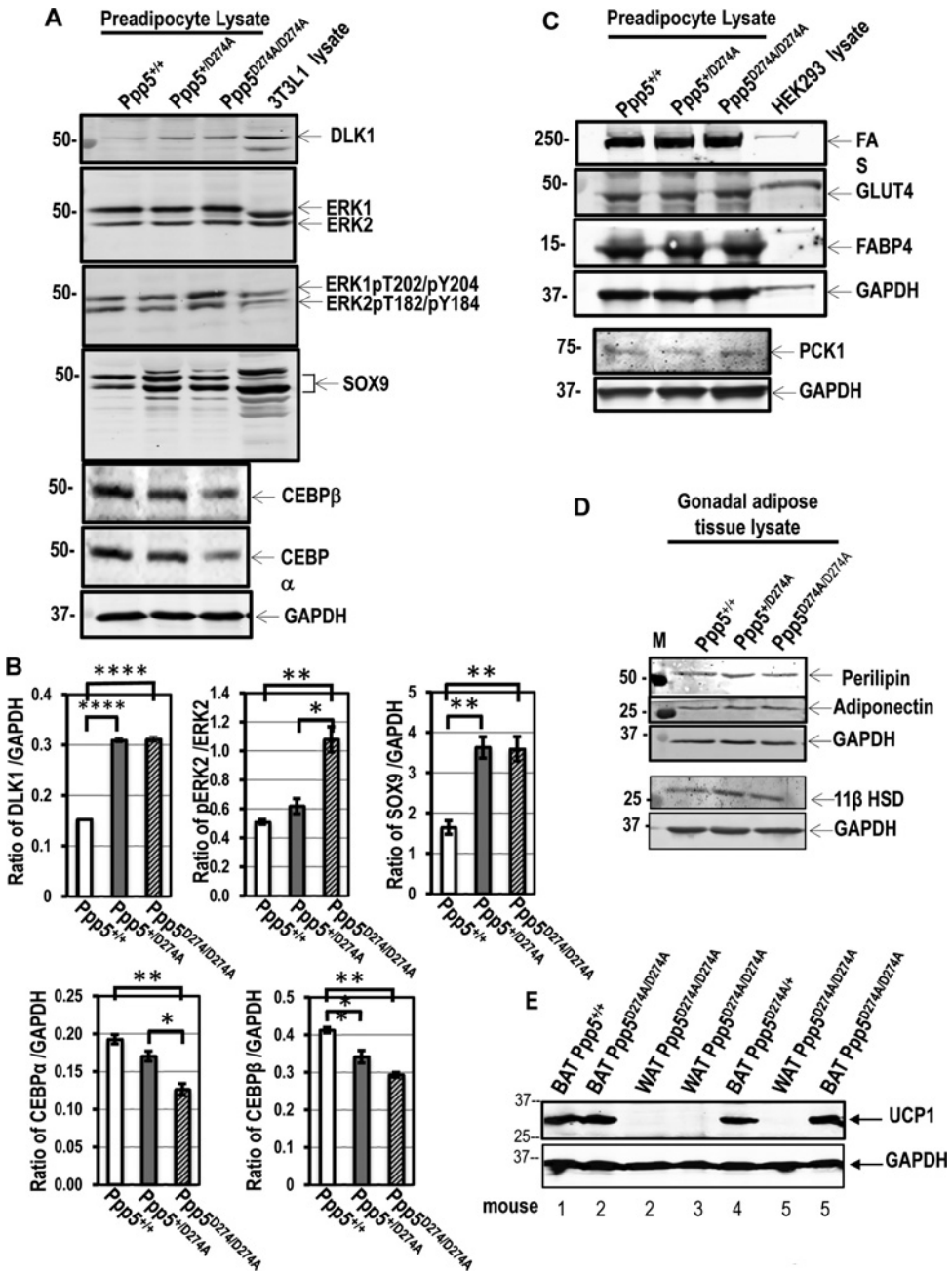

Figure 6 Investigation of proteins regulating preadipocyte differentiation and other processes in gonadal adipose tissue

(**A–C**) Lysates of preadipocytes cultured in DMEM and dialysed FBS. (**A**) Immunoblotting of proteins regulating adipogenesis. Lysates of human 3T3L1 cells facilitate identification of the mouse preadipocyte proteins. The concentrations of DLK1 and SOX9 are increased in $Ppp5^{D274\,A/+}$ and $Ppp5^{D274A/D274A}$ compared with $Ppp5^{+/+}$ cell lysates. ERK2 phosphorylation on Thr182 and Tyr184 is increased in $Ppp5^{D274A/D274A}$ compared with $Ppp5^{+/+}$ lysates. CEBPβ and CEBPα are decreased in $Ppp5^{D274\,A/+}$ and $Ppp5^{D274A/D274A}$ compared with $Ppp5^{+/+}$ lysates. GAPDH from the same mouse lysates serves as a control for equal loading of the samples. The position of the marker proteins in kDa is shown on the left. Representative blots of independent experiments are shown. (**B**) Quantification of immunoblotting data in (**A**) with respect to the concentration of GAPDH. The results are averaged from three independent experiments employing preadipocyte cultures from different mice for each genotype, $^{*}P < 0.02$, $^{**}P < 0.005$, $^{***}P < 0.001$, $^{****}P < 10^{-6}$. (**C**) Immunoblotting of preadipocyte lysates for proteins regulating glucose and fatty acid metabolism. GAPDH from the same mouse lysates serves as a control for equal loading of the samples. HEK293 lysate facilitates identification of the preadipocyte proteins. Marker proteins in kDa are indicated on the left. (**D**) Lysates of gonadal adipose tissue lysate were immunoblotted for the indicated proteins. M, marker proteins in kDa. (**E**) Immunoblotting of lysates from interscapular brown adipose tissue (BAT) and white gonadal tissue (WAT) for UCP1. The UCP1 protein band was blocked by a specific blocking peptide (data not shown). The GAPDH control for loading was detected on the same blot subsequent to UCP1 detection and at a different wavelength by Li-Cor Odyssey software. Maximum loading (50 μg protein) was carried out to determine whether UCP1 is present in $Ppp5^{D274A/D274A}$ WAT. The tissues were from five different mice as indicated.

important for the transcriptional regulation in human cells (Ser203, Ser211 and Ser226) [33] and in murine cells (Ser212, Ser220 and Ser234, respectively) [34]. In our studies, the GR was hyperphosphorylated at Ser212 and Ser220 in $Ppp5^{D274A/D274A}$ MEFs compared with $Ppp5^{+/+}$ controls, when the MEFs were cultured in DMEM containing dialysed FBS, to remove glucocorticoids. No clear changes were observed in phosphorylation of Ser234, which was difficult to detect (data not shown). Studies in human osteosarcoma cell line U2OS stably expressing human GR and depleted of Ppp5 by

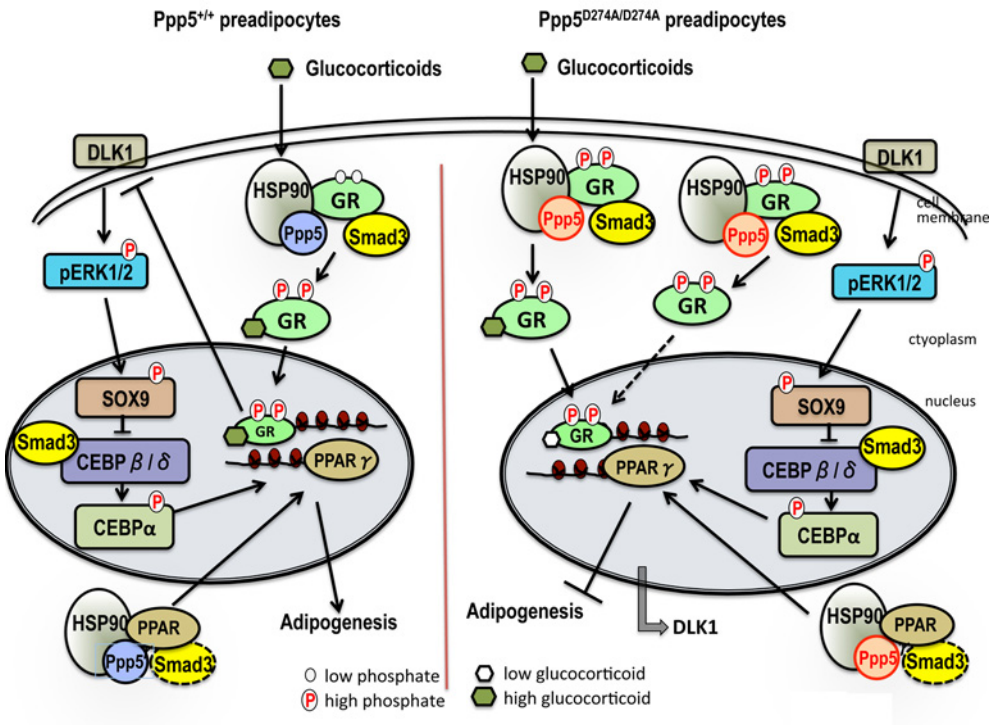

Figure 7 Model comparing the roles of Ppp5 in GR function during initiation of preadipocyte differentiation in Ppp5$^{+/+}$ and Ppp5$^{D274A/D274A}$ mice

Preadipocyte differentiation is inhibited via a 50 kDa factor cleaved from membrane tethered DLK/Pref1, which binds to a receptor leading to phosphorylation and activation of the ERK/MAPK pathway in the cell cytoplasm and SOX9 in the nucleus, blocking the transcription of CEBPβ and CEBPδ (CEBPβ/δ) [36]. In wild-type Ppp5$^{+/+}$ mice, glucocorticoids bind to the GR and Hsp90-Ppp5 is probably replaced by Hsp90-FKBP51 (not shown). Loss of Ppp5 enhances phosphorylation of GRSer212 and GRSer220, and the liganded, phosphorylated GR is imported into the nucleus, where it binds to the promoter of the DLK1 gene, leading to down regulation of DLK1 and initiation of preadipocyte differentiation. CEBP is induced as the levels of CEBPβ and CEBPδ decline, which contributes to the induction of PPARγ necessary for the accumulation of lipid. In Ppp5$^{D274A/D274A}$ mice, the GR is maximally hyperphosphorylated on Ser212 and Ser220 in the absence and presence of interaction with glucocorticoids. The inactive Ppp5 may stay bound to the GR through Hsp90. Hyperphosphorylated GR may not interact optimally with glucocorticoids and some may remain in the unliganded (glucocorticoid free) form, which may not function and/or may block the GR down regulation of DLK1 and thus initiation of adipogenesis. SMAD3 interactions shown do not differ in Ppp5$^{D274A/D274A}$ and Ppp5$^{+/+}$ preadipocytes. Decreasing the glucocorticoid level in preadipocyte cultures (Figure 4C compared with Figure 4B) may increase the unliganded hyper-phoshorylated form of GR in Ppp5$^{D274A/D274A}$ preadipocytes, further decreasing the GR regulated down regulation of DLK1 and adipogenesis. In Ppp5$^{+/+}$ preadipocytes, active Ppp5 keeps unliganded GR dephosphorylated allowing the low levels of glucocorticoid bound GR to inhibit the down-regulation of DLK1 in a few preadipocytes and allow adipogenesis.

siRNA, reported hyperphosphorylation of human GR Ser203 and Ser226 but not Ser211 [16]. It is possible that the use of the osteosarcoma cell line or culture in the presence of complete FBS (which probably contains glucocorticoids) may account for the differences observed at human Ser211 (mouse Ser220) and human Ser226 (mouse Ser234). Addition of dexamethasone to the MEFs in our studies led to hyperphosphorylation of the GR at Ser212 and Ser220 in all three Ppp5 genotypes. Our data therefore suggest that the main role of Ppp5 in regulating the GR is when the GR is in the unliganded state.

The GR interacts with the chaperone Hsp90, which binds the Ppp5 TPR domain via its TPR acceptor site [11,35]. Our studies show that in Ppp5$^{+/+}$ control mice the quantity of Ppp5, which is bound to the GR–Hsp90 complex, decreases when dexamethasone is bound to the GR (Figure 5B), suggesting the role of Ppp5 may be to keep the GR dephosphorylated in the unliganded form (Figure 7). In the Ppp5$^{D274\,A/+}$ and Ppp5$^{D274A/D274A}$ MEFs, where Ppp5 is at least partially inactive, the quantity of Ppp5 bound is more variable.

Although there was a severe decrease in the size of the gonadal and kidney fat pads in Ppp5$^{D274A/D274A}$ mice, preadipocytes could be isolated from these tissues, but after 8–10 days in RPMI medium and FBS, differentiation of the preadipocytes to adipocytes was retarded in Ppp5$^{D274A/D274A}$ and Ppp5$^{D274\,A/+}$ cultures compared with Ppp5$^{+/+}$ cultures, pointing to a major defect in preadipocyte differentiation in Ppp5 deficient mice. Previous studies examined PP5KO MEFs cultured in a medium to force conversion into adipocytes [DMEM, 10 % FBS, 1 μM dexamethasone, 830 nM insulin, 100 μM isobutylmethylxanthine, 5 μM rosiglitazone (an agonist of PPARγ)] [23]. The authors observed that the abundance of cells with lipid accumulation was lower in PP5KO compared with the PP5WT (wild-type) cells. However, the GR was reported to be hyperphosphorylated in PP5KO MEFs when activated by dexamethasone and the PPARγ2 (transfected into the MEFs) hyperphosphorylated on Ser112 with inactivation. The abrogation of PPARγ activity was described as the dominant mechanism preventing lipid accumulation in PP5KO MEFs. This contrasts with our study, which shows clear differences in GR phosphorylation in the unliganded form in MEFs and no changes in endogenous PPARγ Ser112 phosphorylation in gonadal fat pads.

The transmembrane protein DLK1/Pref1/FA1, with six EGF (epidermal growth factor)-like repeats on the extracellular domain, has been recognized as a crucial factor in the differentiation of preadipocytes to mature adipocytes [36]. Tumour necrosis factor-α (TNF-α) converting enzyme (TACE) is reported to cleave DLK1, generating a 50 kDa soluble extracellular form, which interacts with fibronectin and the cell membrane protein integrin $\alpha5\beta1$, leading to activation of an ERK/MAPK, SOX9 pathway to block CEBPβ/δ transcription

and adipocyte differentiation. Dexamethasone was shown to decrease DLK1 expression, allowing an increase of CEBPβ/δ and adipocyte differentiation [25]. Our studies show that after culture of preadipocytes in RPMI medium and dialysed FBS (to remove glucocorticoids), DLK1 and SOX9 protein concentrations are higher in $Ppp5^{D274\,A/+}$ and $Ppp5^{D274A/D274A}$ than in $Ppp5^{+/+}$ cultures, resulting in lower expression levels of the CEBPβ. CEBPα, which is induced by CEBPβ, therefore exhibits lower expression levels. No comparable studies on the proteins regulating the pathways of adipogenesis were performed in mouse PP5KO models [17,18,23].

As the major phenotype of $Ppp5^{D274A/D274A}$ mice was observed in adipose tissue, several proteins were examined in gonadal fat pad or preadipocyte lysates. However, we observed no difference in the concentration of 11-β-HSD1, which converts the inactive 11-dehydrocorticosterone (cortisone in humans) into active corticosterone (cortisol in humans) [37]. There was also no alteration in adiponectin, involved in the modulation of lipid and glucose metabolism in insulin sensitive tissues [38], PEPCK a major regulator in gluconeogenesis, dependent on binding of the GR to DNA for induction [39], FABP4 [40] and perilipin, [41], which mediate transport and release of fatty acids, respectively. The concentration of FAS, a rate-limiting enzyme of fatty acid synthesis, was also similar in $Ppp5^{D274A/D274A}$, $Ppp5^{D274\,A/+}$ and $Ppp5^{+/+}$ mice. The more variable levels of GLUT4, which were sometimes, but not always, raised in $Ppp5^{D274A/D274A}$ preadipocytes, may be a compensatory response to low lipid levels and account for the slightly increased insulin sensitivity of the mice in $Ppp5^{D274A/D274A}$ preadipocytes. The decreased lipid in gonadal and peri-renal fat pads raised the possibility that dietary fat was being stored in other tissues, but the hepatic lipid levels of $Ppp5^{D274A/D274A}$ mice were not elevated, providing no evidence for excess fat deposition in this tissue.

Our studies show an interaction of SMAD3 with GR–Hsp90–Ppp5 complexes consistent with previous studies using cell lines, which also showed that the transcriptional activation function of SMAD3 was inhibited by a mechanism dependent on interaction with the GR [24]. Molecular modelling has suggested that phosphorylation of the GR at Ser211 promotes a conformational change, which may enhance interaction with certain proteins [42], but we found no evidence for differences in SMAD3 binding to the GR in preadipocytes from $Ppp5^{D274A/D274A}$, $Ppp5^{D274\,A/+}$ and $Ppp5^{+/+}$ mice, although the levels of GRpSer212 and GRpSer220 differed in the three genotypes. We observed that SMAD3 also interacted with PPARγ–Hsp90 complexes in preadipocytes. SMAD3 has been shown to interact with CEBPβ/CEBPδ complexes with inhibition of their transcriptional activity [43,44]. A weak interaction of SMAD3 with PPARγ was also observed in these studies, but no evidence for PPARγ inhibition. Therefore, although our data point to an additional role of Ppp5 in PPARγ function, we have no evidence that interactions with SMAD3 are different in $Ppp5^{+/+}$, $Ppp5^{D274\,A/+}$ and $Ppp5^{D274A/D274A}$ mice. Our data show that Ppp5 plays a key role in keeping the unliganded (glucocorticoid-free) GR dephosphorylated at Ser212 and Ser220, which appears to be essential for GR-mediated repression of DLK1, a process required for the initiation of differentiation in proliferating preadipocytes. Other recent studies have provided evidence that the unliganded form of the GR may be crucial for some GR functions [45,46]. The decreased body mass of the $Ppp5^{D274A/D274A}$ mice compared with $Ppp5^{+/+}$ mice cannot be explained solely by a GR-mediated decrease in adipogenesis, but necessitates a change in energy balance. An examination of food intake and the generation of heat through the expression levels of UCP1 in interscapular BAT uncovered no differences between $Ppp5^{D274A/D274A}$ and $Ppp5^{+/+}$ mice. There has been much recent interest in brite or beige adipocytes developing in WAT, as they may play an important role in mice losing weight through elevation of UCP1, which can occur following cold or β-adrenergic stimulation [47]. However, we found no evidence for the existence of UCP1 in gonadal WAT of several $Ppp5^{D274A/D274A}$ mice. Therefore, at the present time it is unclear how the energy intake and expenditure are balanced, but glucocorticoids have wide ranging metabolic effects which may individually be hard to detect.

$Ppp5^{D274A/D274A}$ mice exhibited slightly improved GTT and insulin sensitivity compared with $Ppp5^{+/+}$ mice on a standard control diet. During the course of our studies, it was reported that PP5KO mice showed improved GTT but no increase in insulin sensitivity [48]. Recent studies from the same group report that PP5KO mice fed a control diet exhibit decreased kidney, epididymal and subcutaneous fat depots [49], consistent with our analyses of Ppp5KI mice by weighing and MRI of kidney and gonadal fat depots. Feeding a HFD (45%) for 20 weeks increased weight gain, lowered GTT and led to insulin resistance in Ppp5KI mice and controls. In contrast, PP5KO mice fed a HFD (60%) for 10 weeks, gained less weight and maintained improved GTT compared with control mice after the same HFD. The differences may arise from the different length and composition of the HFDs or possibly the use of Cre/loxP technology to generate the PP5KO mice [18], which has been questioned recently in relation to metabolic phenotypes [50]. In addition, deletion of Ppp5 protein in KO mice may allow a different phosphatase to partially or fully substitute for Ppp5. There can be a problem in interpreting results from KO mice, in which both regulatory and catalytic domains are deleted. Analysing a KI model, like $Ppp5^{D274\,A}$, in which a single functional domain of the protein is disabled, may lead to better prediction of the consequences that could arise from administration of an inhibitor of catalytic function.

Overall our data provide clear evidence that inactivation of Ppp5 *in vivo* in the presence of normal or 2-fold elevation of blood serum glucocorticoid levels partially inhibits preadipocyte differentiation and that $Ppp5^{D274A/D274A}$ mice on a standard diet show increased insulin sensitivity. Initial studies (Doron Rosenzweig, Wright Jacob and Patricia T.W. Cohen – unpublished) have not uncovered significant altered immunological responses in macrophages from $Ppp5^{D274A/D274A}$ compared with $Ppp5^{+/+}$ mice. Therefore, although inhibition of Ppp5 is unlikely to decrease existing visceral obesity, decreasing Ppp5 activity may be beneficial to prevent obesity during glucocorticoid treatment, if inhibition of other reported roles of Ppp5 is not detrimental.

AUTHOR CONTRIBUTION

Wright Jacob carried out the experiments in Figures 2, 3, 4A–4C, 4E, 4F, 5, 6A–6D and S2 and contributed to Figure 7. Doron Rosenzweig contributed to Figure 1D and carried out the experimnts in Figures 1E, 4D, S1D and S3. Cristina Vazquez-Martin contributed to Figure 1D and carried out the experiments in Figures S1A–S1C. Suzanne Duce supervised the MRI experiments, analysis and presentation of the MRI data. Tricia Cohen planned the research, designed the mouse KI mutation Figure 1A, analysed the data for Figures S1B, S1C, S1E and S1F, performed the experiments in Figures 6E and S1G, contributed to Figure 7, collated and analysed the overall results and wrote the paper.

FUNDING

The studies were funded by the Medical Research Council U.K. [grant number G0901221 to P.T.W.C. and pharmaceutical companies supporting the Division of Signal Transduction Therapy (AstraZeneca, Boehringer-Ingelheim, GlaxoSmithKline, Merck KgaA, Janssen Pharmaceutica and Pfizer). S.L.D. gratefully acknowledges financial support from the

Wellcome Trust for her Career Re-entry Fellowship [grant number WT081039] and the Strategic Award [grant number 083481] to the Division of Biological Chemistry and Drug Discovery for IT infrastructure support.

REFERENCES

1 Pratt, W.B. and Toft, D.O. (1997) Steroid receptor interactions with heat shock protein and immunophilin chaperones. Endocr. Rev. **18**, 306–360 PubMed

2 Chen, M.X., McPartlin, A.E., Brown, L., Chen, Y.H., Barker, H.M. and Cohen, P. T. W. (1994) A novel human protein serine/threonine phosphatase which possesses four tetratricopeptide repeat motifs and localizes to the nucleus. EMBO J. **13**, 4278–4290 PubMed

3 Chinkers, M. (1994) Targeting of a distinctive protein-serine phosphatase to the protein kinase- like domain of the atrial natriuretic peptide receptor. Proc. Natl. Acad. Sci. U.S.A. **91**, 11075–11079 CrossRef PubMed

4 Chen, M.-S., Silverstein, A.M., Pratt, W.B. and Chinkers, M. (1996) The tetratricopeptide repeat domain of protein phosphatase 5 mediates binding to glucocorticoid receptor heterocomplexes and acts as a dominant negative mutant. J. Biol. Chem. **271**, 32315–32320 CrossRef PubMed

5 Silverstein, A.M., Galigniana, M.D., Chen, M.-S., Owens-Grillo, J.K., Chinkers, M. and Pratt, W.B. (1997) Protein phosphatase 5 is a major component of glucocorticoid receptor-hsp90 complexes with properties of an FK506-binding immunophilin. J. Biol. Chem. **272**, 16224–16230 CrossRef PubMed

6 Chinkers, M. (2001) Protein phosphatase 5 in signal transduction. Trends Endocrinol. Metab. **12**, 28–32 CrossRef PubMed

7 Zeke, T., Morrice, N., Vázquez-Martin, C. and Cohen, P. T. W. (2005) Human protein phosphatase 5 dissociates from heat-shock proteins and is proteolytically activated in response to arachidonic acid and the microtubule-depolymerizing drug nocodazole. Biochem. J. **385**, 45–56 CrossRef PubMed

8 Heitzer, M.D., Wolf, I.M., Sanchez, E.R., Witchel, S.F. and DeFranco, D.B. (2007) Glucocorticoid receptor physiology. Rev. Endocr. Metab. Disord. **8**, 321–330 CrossRef PubMed

9 Banerjee, A., Periyasamy, S., Wolf, I.M., Hinds, T.D., Jr., Yong, W., Shou, W. and Sanchez, E.R. (2008) Control of glucocorticoid and progesterone receptor subcellular localization by the ligand-binding domain is mediated by distinct interactions with tetratricopeptide repeat proteins. Biochemistry **47**, 10471–10480 CrossRef PubMed

10 Grad, I., McKee, T.A., Ludwig, S.M., Hoyle, G.W., Ruiz, P., Wurst, W., Floss, T., Miller, C.A. and Picard, D. (2006) The Hsp90 cochaperone p23 is essential for perinatal survival. Mol. Cell. Biol. **26**, 8976–8983 CrossRef PubMed

11 Yang, J., Roe, S.M., Cliff, M.J., Williams, M.J., Ladbury, M.A., Cohen, P. T. W. and Barford, D. (2005) Molecular basis for TPR domain-mediated regulation of protein phosphatase 5. EMBO J. **24**, 1–10 CrossRef PubMed

12 Chen, M.X. and Cohen, P. T. W. (1997) Activation of protein phosphatase 5 by limited proteolysis or the binding of fatty acids to the TPR domain. FEBS Lett. **400**, 136–140 CrossRef PubMed

13 Skinner, J., Sinclair, C., Romeo, C., Armstrong, D., Charbonneau, H. and Rossie, S. (1997) Purification of a fatty acid-stimulated protein-serine/threonine phosphatase from bovine brain and its identification as a homolog of protein phosphatase 5. J. Biol. Chem. **272**, 22464–22471 CrossRef PubMed

14 Ramsey, A.J. and Chinkers, M. (2002) Identification of potential physiological activators of protein phosphatase 5. Biochemistry **41**, 5625–5632 CrossRef PubMed

15 Zuo, Z., Urban, G., Scammell, J.G., Dean, N.M., McLean, T.K., Aragon, I. and Honkanen, R.E. (1999) Ser/Thr protein phosphatase type 5 (PP5) is a negative regulator of glucocorticoid receptor-mediated growth arrest. Biochemistry **38**, 8849–8857 CrossRef PubMed

16 Wang, Z., Chen, W., Kono, E., Dang, T. and Garabedian, M.J. (2007) Modulation of glucocorticoid receptor phosphorylation and transcriptional activity by a C-terminal-associated protein phosphatase. Mol. Endocrinol. **21**, 625–634 CrossRef PubMed

17 Yong, W., Bao, S., Chen, H., Li, D., Sanchez, E.R. and Shou, W. (2007) Mice lacking protein phosphatase 5 are defective in ataxia telangiectasia mutated (ATM)-mediated cell cycle arrest. J. Biol. Chem. **282**, 14690–14694 CrossRef PubMed

18 Amable, L., Grankvist, N., Largen, J.W., Ortsater, H., Sjoholm, A. and Honkanen, R.E. (2011) Disruption of serine/threonine protein phosphatase 5 (PP5:PPP5 c) in mice reveals a novel role for PP5 in the regulation of ultraviolet light-induced phosphorylation of serine/threonine protein kinase Chk1 (CHEK1). J. Biol. Chem. **286**, 40413–40422 CrossRef PubMed

19 Chazenbalk, G., Bertolotto, C., Heneidi, S., Jumabay, M., Trivax, B., Aronowitz, J., Yoshimura, K., Simmons, C.F., Dumesic, D.A. and Azziz, R. (2011) Novel pathway of adipogenesis through cross-talk between adipose tissue macrophages, adipose stem cells and adipocytes: evidence of cell plasticity. PLoS One **6**, e17834 CrossRef PubMed

20 Egloff, M.-P., Johnson, F., Moorhead, G., Cohen, P. T. W., Cohen, P. and Barford, D. (1997) Structural basis for the recognition of regulatory subunits by the catalytic subunit of protein phosphatase 1. EMBO J. **16**, 1876–1887 CrossRef PubMed

21 Vaughan, C.K., Mollapour, M., Smith, J.R., Truman, A., Hu, B., Good, V.M., Panaretou, B., Neckers, L., Clarke, P.A., Workman, P. et al. (2008) Hsp90-dependent activation of protein kinases is regulated by chaperone-targeted dephosphorylation of Cdc37. Mol. Cell **31**, 886–895 CrossRef PubMed

22 Spiegelman, B.M. (1998) PPAR-gamma: adipogenic regulator and thiazolidinedione receptor. Diabetes **47**, 507–514 CrossRef PubMed

23 Hinds, T.D. Jr., Stechschulte, L.A., Cash, H.A., Whisler, D., Banerjee, A., Yong, W., Khuder, S.S., Kaw, M.K., Shou, W., Najjar, S.M. and Sanchez, E.R. (2011) Protein phosphatase 5 mediates lipid metabolism through reciprocal control of glucocorticoid receptor and peroxisome proliferator-activated receptor-gamma (PPARgamma). J. Biol. Chem. **286**, 42911–42922 CrossRef PubMed

24 Song, C.Z., Tian, X. and Gelehrter, T.D. (1999) Glucocorticoid receptor inhibits transforming growth factor-beta signaling by directly targeting the transcriptional activation function of Smad3. Proc. Natl. Acad. Sci. U.S.A. **96**, 11776–11781 CrossRef PubMed

25 Smas, C.M., Chen, L., Zhao, L., Latasa, M.J. and Sul, H.S. (1999) Transcriptional repression of pref-1 by glucocorticoids promotes 3T3-L1 adipocyte differentiation. J. Biol. Chem. **274**, 12632–12641 CrossRef PubMed

26 Tomlinson, J.J., Boudreau, A., Wu, D., Atlas, E. and Hache, R.J. (2006) Modulation of early human preadipocyte differentiation by glucocorticoids. Endocrinology **147**, 5284–5293 CrossRef PubMed

27 Kim, K.A., Kim, J.H., Wang, Y. and Sul, H.S. (2007) Pref-1 (preadipocyte factor 1) activates the MEK/extracellular signal-regulated kinase pathway to inhibit adipocyte differentiation. Mol. Cell. Biol. **27**, 2294–2308 CrossRef PubMed

28 Wang, Y. and Sul, H.S. (2009) Pref-1 regulates mesenchymal cell commitment and differentiation through Sox9. Cell Metab. **9**, 287–302 CrossRef PubMed

29 Yeh, W.C., Cao, Z., Classon, M. and McKnight, S.L. (1995) Cascade regulation of terminal adipocyte differentiation by three members of the C/EBP family of leucine zipper proteins. Genes Dev. **9**, 168–181 CrossRef PubMed

30 Farmer, S.R. (2006) Transcriptional control of adipocyte formation. Cell Metab. **4**, 263–273 CrossRef PubMed

31 Soumano, K., Desbiens, S., Rabelo, R., Bakopanos, E., Camirand, A. and Silva, J.E. (2000) Glucocorticoids inhibit the transcriptional response of the uncoupling protein-1 gene to adrenergic stimulation in a brown adipose cell line. Mol. Cell. Endocrinol. **165**, 7–15 CrossRef PubMed

32 Cole, T.J., Blendy, J.A., Monaghan, A.P., Krieglstein, K., Schmid, W., Aguzzi, A., Fantuzzi, G., Hummler, E., Unsicker, K. and Schutz, G. (1995) Targeted disruption of the glucocorticoid receptor gene blocks adrenergic chromaffin cell development and severely retards lung maturation. Genes Dev. **9**, 1608–1621 CrossRef PubMed

33 Almlof, T., Wright, A.P. and Gustafsson, J.A. (1995) Role of acidic and phosphorylated residues in gene activation by the glucocorticoid receptor. J. Biol. Chem. **270**, 17535–17540 CrossRef PubMed

34 Webster, J.C., Jewell, C.M., Bodwell, J.E., Munck, A., Sar, M. and Cidlowski, J.A. (1997) Mouse glucocorticoid receptor phosphorylation status influences multiple functions of the receptor protein. J. Biol. Chem. **272**, 9287–9293 CrossRef PubMed

35 Sanchez, E.R. (2012) Chaperoning steroidal physiology: Lessons from mouse genetic models of Hsp90 and its cochaperones. Biochim. Biophys. Acta **1823**, 722–729 CrossRef PubMed

36 Hudak, C.S. and Sul, H.S. (2013) Pref-1, a gatekeeper of adipogenesis. Front. Endocrinol. (Lausanne) **4**, 79 PubMed

37 van Raalte, D.H., Ouwens, D.M. and Diamant, M. (2009) Novel insights into glucocorticoid-mediated diabetogenic effects: towards expansion of therapeutic options? Eur. J. Clin. Invest. **39**, 81–93 CrossRef PubMed

38 Chandran, M., Phillips, S.A., Ciaraldi, T. and Henry, R.R. (2003) Adiponectin: more than just another fat cell hormone? Diabetes Care **26**, 2442–2450 CrossRef PubMed

39 Reichardt, H.M., Kaestner, K.H., Tuckermann, J., Kretz, O., Wessely, O., Bock, R., Gass, P., Schmid, W., Herrlich, P., Angel, P. and Schutz, G. (1998) DNA binding of the glucocorticoid receptor is not essential for survival. Cell **93**, 531–541 CrossRef PubMed

40 Kazantzis, M. and Stahl, A. (2012) Fatty acid transport proteins, implications in physiology and disease. Biochim. Biophys. Acta **1821**, 852–857 CrossRef PubMed

41 Tansey, J.T., Sztalryd, C., Gruia-Gray, J., Roush, D.L., Zee, J.V., Gavrilova, O., Reitman, M.L., Deng, C.X., Li, C., Kimmel, A.R. and Londos, C. (2001) Perilipin ablation results in a lean mouse with aberrant adipocyte lipolysis, enhanced leptin production, and resistance to diet-induced obesity. Proc. Natl. Acad. Sci. U.S.A. **98**, 6494–6499 CrossRef PubMed

42 Chen, W., Dang, T., Blind, R.D., Wang, Z., Cavasotto, C.N., Hittelman, A.B., Rogatsky, I., Logan, S.K. and Garabedian, M.J. (2008) Glucocorticoid receptor phosphorylation differentially affects target gene expression. Mol. Endocrinol. **22**, 1754–1766 CrossRef PubMed

43 Choy, L. and Derynck, R. (2003) Transforming growth factor-beta inhibits adipocyte differentiation by Smad3 interacting with CCAAT/enhancer-binding protein (C/EBP) and repressing C/EBP transactivation function. J. Biol. Chem. **278**, 9609–9619 CrossRef PubMed
44 Rosen, E.D. and MacDougald, O.A. (2006) Adipocyte differentiation from the inside out. Nat. Rev. Mol. Cell Biol. **7**, 885–896 CrossRef PubMed
45 Grad, I. and Picard, D. (2007) The glucocorticoid responses are shaped by molecular chaperones. Mol. Cell. Endocrinol. **275**, 2–12 CrossRef PubMed
46 Bouazza, B., Debba-Pavard, M., Amrani, Y., Isaacs, L., O'Connell, D., Ahamed, S., Formella, D. and Tliba, O. (2013) Basal p38 MAPK regulates unliganded glucocorticoid receptor function in airway smooth muscle cells. Am. J. Respir. Cell Mol. Biol. **50**, 301–315
47 Beranger, G.E., Karbiener, M., Barquissau, V., Pisani, D.F., Scheideler, M., Langin, D. and Amri, E.Z. (2013) In vitro brown and "brite"/"beige" adipogenesis: human cellular models and molecular aspects. Biochim. Biophys. Acta **1831**, 905–914 CrossRef PubMed
48 Grankvist, N., Amable, L., Honkanen, R.E., Sjoholm, A. and Ortsater, H. (2012) Serine/threonine protein phosphatase 5 regulates glucose homeostasis in vivo and apoptosis signalling in mouse pancreatic islets and clonal MIN6 cells. Diabetologia **55**, 2005–2015 CrossRef PubMed
49 Grankvist, N., Honkanen, R.E., Sjoholm, A. and Ortsater, H. (2013) Genetic disruption of protein phosphatase 5 in mice prevents high-fat diet feeding-induced weight gain. FEBS Lett. **587**, 3869–3874 CrossRef PubMed
50 Harno, E., Cottrell, E.C. and White, A. (2013) Metabolic pitfalls of CNS Cre-based technology. Cell Metab. **18**, 21–28 CrossRef PubMed

Received 3 April 2014/19 November 2014; accepted 1 December 2014
Published as BJ Immediate Publication 1 December 2014, doi:10.1042/BJ20140428